Journal of Pharmaceutical Analysis 12 (2022) 415–423

Contents lists available at ScienceDirect

Journal of Pharmaceutical Analysis

journal homepage: www.elsevier.com/locate/jpa

Original article

A preparation strategy for protein-oriented immobilized silica magnetic beads with Spy chemistry for ligand fishing

Yu Yi*, Jianming Hu, Shenwei Ding, Jianfeng Mei, Xudong Wang, Yanlu Zhang, Jianshu Chen, Guoqing Ying**

Institute of Biopharmaceuticals, College of Pharmaceutical Science, Zhejiang University of Technology, Hangzhou, 310014, China

ARTICLE INFO

Article history:
Received 7 April 2021
Received in revised form
18 July 2021
Accepted 24 July 2021
Available online 26 July 2021

Keywords:
EDC/Sulfo-NHS
SpyTag/SpyCatcher
Green fluorescent protein
Silica magnetic beads
Oriented immobilization
Drug screening

ABSTRACT

Due to the complexity of bioactive ingredients in biological samples, the screening of target proteins is a complex process. Herein, a feasible strategy for directing protein immobilization on silica magnetic beads for ligand fishing based on SpyTag/SpyCatcher (ST/SC)-mediated anchoring is presented. Carboxyl functional groups on the surface of silica-coated magnetic beads (SMBs) were coupled with SC using the 1-ethyl-3-(3-dimethylaminopropyl) carbodiimide hydrochloride/*N*-hydroxysulfosuccinimide method, named SC-SMBs. The green fluorescent protein (GFP), as the capturing protein model, was ST-labeled and anchored at a specific orientation onto the surface of SC-SMBs directly from relevant cell lysates via ST/SC self-ligation. The characteristics of the SC-SMBs were studied via electron microscopy, energy dispersive spectroscopy, and Fourier transform infrared spectroscopy. The spontaneity and site-specificity of this unique reaction were confirmed via electrophoresis and fluorescence analyses. Although the alkaline stability of ST-GFP-ligated SC-SMBs was not ideal, the formed isopeptide bond was unbreakable under acidic conditions (0.05 M glycine-HCl buffer, pH 1–6) for 2 h, under 20% ethanol solution within 7 days, and at most temperatures. We, therefore, present a simple and universal strategy for the preparation of diverse protein-functionalized SMBs for ligand fishing, prompting its usage on drug screening and target finding.

1. Introduction

The identification of target bioactive ingredients from crude extracts and complex matrices, including biological samples, is laborious and time-consuming. This is due to the wide range of dynamic contents in metabolites and bioactive macromolecules, which typically require additional enrichment and/or purification steps [1]. Numerous advanced screening methods have emerged in the past decades [2,3], including ligand fishing, where a protein is immobilized onto the surface of a magnetic bead and used to screen complex matrices [4–11]. After immobilizing a bait protein, the resulting stationary phase can be used to specifically capture the target bioactive ingredients from complex matrices through a simple incubation, relying on the affinity of ligand-protein binding. Considering the solid-liquid separation procedure after capture, silica-coated magnetic beads (SMBs) [4–9] are suitable carriers for ligand fishing. The advantage of magnetic beads is that magnetic separation is gentle and non-destructive to the captured target protein, thereby fully preserving its activity. Meanwhile, the surface of SMBs can be easily modified with various functional groups [4,5,7], such as carboxyl [10] or amine groups [11], which are very useful for conjugating a particular protein with suitable cross-linking agents [7] (e.g., glutaraldehyde [4,5] and carbodiimide [5]). However, these chemical conjugations can result in proteins being immobilized stochastically, if not controlled by external factors such as pH [12]. Furthermore, while the majority of these immobilizations are carried out straightforwardly under mild conditions [4,5], some require multiple steps [13–16] to acquire higher site-specificity. Immobilization using bioaffinity-specific interactions, such as the avidin-biotin system [17], His-tag system [18], and protein A/protein G system [19], also offers gentle conditions in addition to target-specific protein immobilization. However, in this case, most of these reactions are noncovalent and reversible, which can result in protein loss under certain circumstances. Another problem is that distinct purification procedures must be designed

Peer review under responsibility of Xi'an Jiaotong University.
* Corresponding author.
** Corresponding author.
E-mail addresses: yiyu1106@zjut.edu.cn (Y. Yi), gqying@zjut.edu.cn (G. Ying).

https://doi.org/10.1016/j.jpha.2021.07.008

for the diverse capturing proteins used, where the entire purification process is tedious and time-consuming.

Recently, a novel self-ligating system, the SpyTag/SpyCatcher (ST/SC) system, has attracted considerable interest [20–22]. Howarth and co-workers [20,23] split and engineered the second immunoglobulin-like collagen adhesin domain of fibronectin-binding protein, which originated from *Streptococcus pyogenes*, into two peptide fragments, ST and SC. Once mixed, the reactive Asp117 in ST (13 amino acids long) spontaneously forms an isopeptide bond with the reactive Lys31 in SC (116 amino acids long), as promoted by Glu77 in SC. It was found that the isopeptide bond formed was covalent, irreversible, and chemically stable as a typical amide bond [24]. The bond formation process was not only efficient but also nearly quantitative under diverse reaction conditions, such as a broad range of pH values (5–8), temperatures (4–37 °C), buffers, redox environments, and non-ionic detergents [20]. Most importantly, the ST/SC system is fully genetically encoded, and the reaction will still occur efficiently at the locations where ST or SC is embedded [20,25] as long as there are no steric hindrances. To date, the bioconjugation between ST and SC has been observed to be site-specific in vitro using cells from various species [26]. It was also confirmed that ST/SC-mediated anchoring retained a precise spatial orientation [27,28].

Considering that the ST/SC self-ligating system is carried out under mild conditions, and the formed isopeptide bond results in an oriented protein immobilization and is much more stable than noncovalent binding, we designed a simple strategy for directed protein immobilization on SMBs using ST/SC-mediated anchoring for ligand fishing. The SC protein was expressed, purified, and immobilized onto the surfaces of carboxyl SMBs using the 1-ethyl-3-[3-dimethylaminopropyl] carbodiimide hydrochloride/*N*-hydroxysulfosuccinimide (EDC/Sulfo-NHS) [29] method. The SC-SMBs were characterized via scanning electron microscopy (SEM), transmission electron microscopy (TEM), energy dispersive spectroscopy (EDS), and Fourier transform infrared (FT-IR) spectroscopy. Green fluorescent protein (GFP) was chosen as a model that represented active capturing protein, with a SpyTag label at its N-terminus (ST-GFP). Subsequently, the fusion protein ST-GFP was expressed, directly captured from crude cell lysate supernatants, and immobilized in a specific orientation onto SC-SMBs, resulting in ST-GFP@SC-SMBs. The lysine-selective binding specificity of SC-SMBs to ST-GFP was examined via comparison with that of bovine serum albumin (BSA)-SMBs. The alkaline stability, acidic pH stability, storage stability, and temperature stability of ST-GFP@SC-SMBs were also evaluated.

The strategy of this uniquely oriented covalent self-ligating reaction can avoid potential issues in covalent immobilization and/or bioaffinity-specific interactions, resulting in the increased capturing capacity of protein-functionalized SMBs. In addition, this strategy took advantage of the universality of SC-SMB modules, which could directly and selectively bind ST-labeled capturing proteins from cell lysates, avoiding the need for purification procedures in preparing capturing proteins for immobilization. Since SC is the only protein that needs to be purified, its purification procedure and coupling process to SMBs can be easily standardized and scaled up. These advantages simplify the preparation process of protein-functionalized magnetic beads and guarantee their optimum capturing capacity and reusability for ligand fishing in drug discovery, target finding, and other similar applications. To the best of our knowledge, this is the first report of a ST/SC-mediated anchoring as applied to the preparation of protein-functionalized SMBs for ligand fishing. In addition, the stability of the prepared protein-functionalized beads using this strategy was evaluated in detail, and the specificity of the bioconjugation between SC and ST-GFP was first investigated using BSA in this study.

2. Materials and methods

2.1. Materials

The plasmid pET30a(+)-6× His-SC, pET28a(+)-6× His-ST-GFP, and the competent *Escherichia coli* (*E. coli*) strain BL21(*DE3*) were obtained from our laboratory. $Na_2HPO_4{\cdot}12H_2O$, $NaH_2PO_4{\cdot}2H_2O$, $CaCl_2$, NaCl, HCl, NaOH, and ethanol were purchased from Sinopharm (Beijing, China). EDC, Sulfo-NHS, kanamycin sulfate, agar, isopropyl-β-D-thiogalactopyranoside (IPTG), imidazole, glycine, 2-(*N*-morpholino)ethanesulfonic acid (MES), BSA, SDS-PAGE preparation kit, Bradford reagent, and carboxyl-SMBs (300 nm in diameter) were purchased from Sangon Biotechnology (Shanghai, China). A 0.1 M phosphate-buffered saline solution (PBS, pH 7.4) was prepared with 29 mg/mL $Na_2HPO_4{\cdot}12H_2O$, 2.965 mg/mL $NaH_2PO_4{\cdot}2H_2O$, and 8.766 mg/mL NaCl in distilled water, and the pH was adjusted to 7.4 by 1.0 M HCl. PBS (0.02 M) was prepared with 5.8 mg/mL $Na_2HPO_4{\cdot}12H_2O$, 0.593 mg/mL $NaH_2PO_4{\cdot}2H_2O$, and 29.22 mg/mL NaCl in distilled water, and the pH was adjusted to 7.4 by 1.0 M HCl. HisTrap™ HP 5 mL columns were obtained from GE Healthcare (Pittsburgh, PA, USA). Amicon® Ultra-15 centrifugal filter devices were purchased from Merck Millipore (Darmstadt, Germany).

2.2. Instruments and conditions

Cell disruption was performed using a JY92-IIDN cell disruption ultrasonic homogenizer (Scientz Biotechnology, Ningbo, China). An ÄKTA Purifier-FPLC System (GE, Boston, MA, USA) was utilized for protein purification. A magnetic shelf (Sangon Biotechnology, Shanghai, China) was used to separate the magnetic beads from the liquid suspension. Bradford assay results were measured at 595 nm using a SpectraMax® M5 multi-mode microplate reader (Molecular Devices, Sunnyvale, CA, USA). An S-4800 field emission scanning electron microscope (Hitachi, Tokyo, Japan) with an accelerating voltage of 3 kV and a JEM-1200EX transmission electron microscope (JEOL, Tokyo, Japan) with an accelerating voltage of 100 kV was used to observe the morphologies of the beads. An EMAX 7593-H energy-dispersive X-ray spectrometer (Horiba, Kyoto, Japan) was used for the elemental analyses. FT-IR spectra were obtained using a Nicolet 6700 FT-IR spectrometer (Thermo, Waltham, MA, USA) from the wave numbers 4000 to 400 cm^{-1}. Fluorescence observations and images were obtained using a CKX53

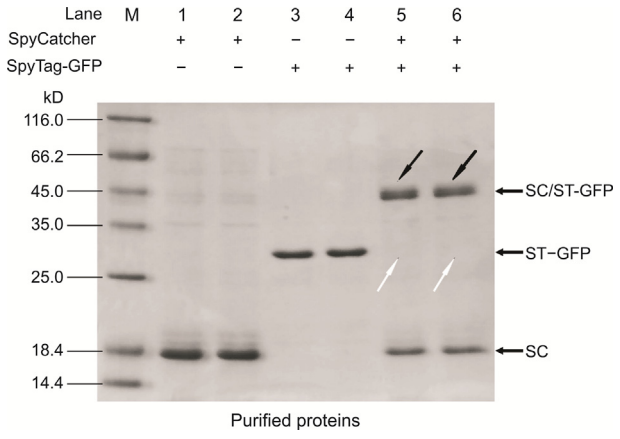

Fig. 1. SDS-PAGE analysis of the reaction between the purified His-tagged SpyCatcher (SC) and SpyTag-green fluorescent protein (ST-GFP) ($n = 2$). Lanes 1 and 2: purified His-tagged SC; lanes 3 and 4: purified His-tagged ST-GFP; lanes 5 and 6: the reaction product between the purified His-tagged SC and ST-GFP.

inverted microscope (Olympus, Tokyo, Japan) with a CKX3-RFA fluorescence illuminator.

2.3. Construction of the expression strains

The plasmids pET30a(+)-6× His-SC and pET28a(+)-6× His-ST-GFP were independently transformed into competent *E. coli* strain BL21(*DE3*) via a $CaCl_2$-mediated heat shock method [30]. The cells were spread onto Luria-Broth (LB)-Kan plates (kanamycin 50 μg/mL) and incubated at 37 °C for 16 h. Positive clones were chosen via colony PCR and were further confirmed via DNA sequencing. The positive transformants were denoted as BL21-SC and BL21-ST-GFP, respectively.

2.4. Induced expressions of recombinant proteins

One positive BL21-SC colony from the screening plate was inoculated into a tube containing 5 mL of LB-Kan medium. The tube was shaken at 180 r/min at 37 °C for 12 h, then 1 mL of this overnight culture was placed in 100 mL of LB-Kan medium and incubated at 37 °C for 2–3 h until the OD_{600} reached 0.6. Afterward, 1 mL of this culture was taken as the uninduced control for the detection of recombinant protein expression via SDS-PAGE with Coomassie staining.

IPTG (100 mM stock solution) was added to the cultures at a final concentration of 0.40 mM, and the conical flasks were shaken for a further 10 h at 180 r/min at 37 °C. The optimal induction conditions for the expression of ST-GFP were 0.40 mM IPTG (final concentration), 180 r/min at 30 °C for 12 h.

One milliliter of the above culture was taken as the post-induction sample for the detection of recombinant protein expression via SDS-PAGE with Coomassie staining. The remaining culture was centrifuged at 8,000 *g* for 5 min at 4 °C, the supernatant was decanted, and then the pellet was resuspended in 5 mL of binding buffer (0.02 M PBS, 5 mM imidazole, pH 7.4) and stored at 4 °C until use.

2.5. Purification of His-tagged SC and ST-GFP

The bacterial suspension was sonicated at 300 W with 2-s action periods and 4-s intervals for 20 min in an ice-water bath. The resulting lysate was then clarified via centrifugation at 10,000 r/min for 10 min at 4 °C. The supernatant was recovered and filtered through a 0.22-μm filter as the cell lysate supernatant before further purification.

The whole purification process was performed on an ÄKTA Purifier. The supernatant was loaded onto a 5 mL HisTrap™ HP column, with a loading volume of 2 mL each time. Next, the column was washed with binding buffer until the absorbance at 280 nm reached a steady baseline (approximately 10 column volumes), proceeding with five column volumes of wash buffer (0.02 M PBS, 30 mM imidazole, pH 7.4). The His-tagged proteins were eluted with the elution buffer (0.02 M PBS, 500 mM imidazole, pH 7.4) using a linear gradient of imidazole (30–400 mM imidazole, 0.02 M PBS, pH 7.4). The eluted proteins were dialyzed with gentle stirring in 0.1 M PBS (pH 7.4) at 4 °C for 6 h each time, three times in total. After imidazole was removed, the dialyzed protein was further concentrated using Amicon® Ultra-15 centrifugal filter devices. The concentrates were collected in 10 mL centrifuge tubes, and the protein concentrations were measured using the Bradford assay with BSA as a standard. The purified proteins were further analyzed via SDS-PAGE and were stored at −20 °C until use.

2.6. Coupling of magnetic beads with His-tagged SC

Carboxyl superparamagnetic SMBs (0.3 μm, 25 mg) were washed three times with an activation buffer (0.1 M MES, 0.5 M NaCl, pH 6.0), and then suspended in a 2 mL-microcentrifuge tube in the same buffer (750 μL). Meanwhile, 50 mg/mL EDC and 50 mg/mL Sulfo-NHS stock solutions were prepared with the activation buffer. EDC (250 μL) and Sulfo-NHS stock solutions (250 μL) were added to the carboxyl magnetic bead suspensions and were incubated at room temperature (25 °C) for 15 min. The beads were separated from the solution using a magnetic shelf. Next, 1 mL of purified His-tagged SC protein was mixed with the activated carboxyl magnetic beads and incubated at 4 °C for 16 h under continuous shaking. After magnetic separation of the beads, the supernatant protein solutions were removed using a pipette and were stored at 4 °C for further concentration measurements. The residual unreacted carboxyl groups on the beads were neutralized with 1.5 mL of blocking buffer (1 M glycine, pH 8.0) under gentle shaking for 30 min. The supernatant was discarded, and the beads were washed again with blocking buffer. Thereafter, the beads were rinsed with preservation buffer (0.1 M PBS, pH 7.4) three times and finally stored at 4 °C in the same buffer (1 mL). Meanwhile, 0.5 mg/mL BSA was coupled with an equal quantity of activated carboxyl magnetic beads via the same procedure for subsequent comparative analyses.

As the volume of protein solution did not change before and after coupling, the coupling efficiency (CE) was calculated

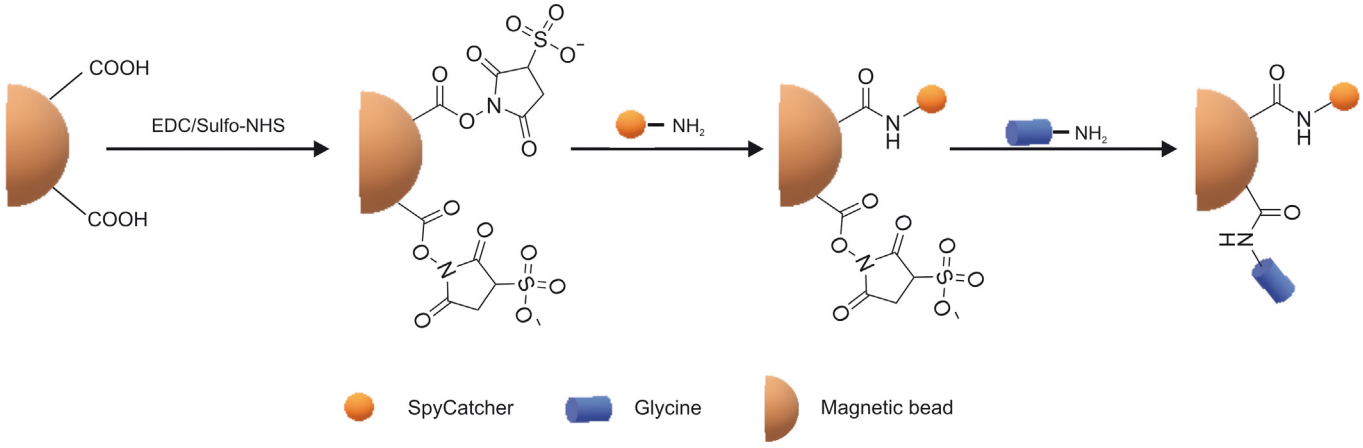

Fig. 2. Schematic representation of the preparation of SC-coupled magnetic beads.

according to the following equation:

$$CE = \frac{c_{Before} - c_{After}}{c_{Before}} \times 100\% \quad (1)$$

Where c_{Before} represents the protein concentration before coupling, and c_{After} is the protein concentration after coupling.

The relative coupling efficiency (RCE) was calculated according to the following equation:

$$RCE\ (mg/g) = \frac{\left(c_{Before} - c_{After}\right) \times V}{m_{Beads}} \quad (2)$$

Where c_{Before} represents the protein concentration before coupling, c_{After} is the protein concentration after coupling, V is the added volume of the protein solution, and m_{Beads} is the weight of the magnetic beads used in grams.

Characterization studies of SC-SMBs were also performed. The surface morphologies of the beads were observed using SEM and TEM. Their EDS were analyzed using an EMAX. The FT-IR spectra of SC protein, SMBs, and SC-SMBs were obtained via FT-IR spectrometry.

2.7. Oriented immobilization of ST-GFP to the coupled magnetic beads

After evenly mixing, 500 μL of SC-SMBs suspended in the preservation buffer were transferred into another tube and kept in reserve, serving as blank control for subsequent fluorescence analyses. The supernatant of the remaining SC-SMB suspensions (500 μL) was removed, and the beads were incubated with 1 mL of cell lysate supernatant containing His-tagged ST-GFP under moderate shaking at room temperature (25 °C) for 12 h. Subsequently, the beads were rinsed with 0.1 M PBS (pH 7.4) three times and stored in the preservation buffer (500 μL) at 4 °C. In parallel, the BSA-coupled magnetic beads (BSA-SMBs) were also incubated with 1 mL of His-tagged ST-GFP cell lysate supernatant and underwent the same rinsing procedure and preservation conditions. After being rinsed with preservation buffer for three times, these beads were analyzed via fluorescence microscopy.

2.8. Stability measurements

The alkaline stability of the ST-GFP-conjugated SC-SMBs (ST-GFP@SC-SMBs) was investigated by measuring the concentration of the proteins detached from the beads after treatment with various concentrations of sodium hydroxide solutions for 2 h. The acidic pH stability of ST-GFP@SC-SMBs was determined by measuring the concentration of the proteins detached from the beads after treatment with 0.05 M glycine-HCl buffer at different pH values for 2 h. Storage stability was also determined by measuring the concentration of the proteins detached from the ST-GFP@SC-SMBs every day upon storage in 20% (*V/V*) ethanol solution for 7 days. The effect of temperature on the stability of ST-GFP@SC-SMBs in 0.1 M PBS (pH 7.4) was also tested by measuring the concentration of the proteins detached from the beads after immersion in a water bath at different temperatures (4, 25, 37, 45, 55, and 65 °C for 2 h, and 100 °C for 10 min).

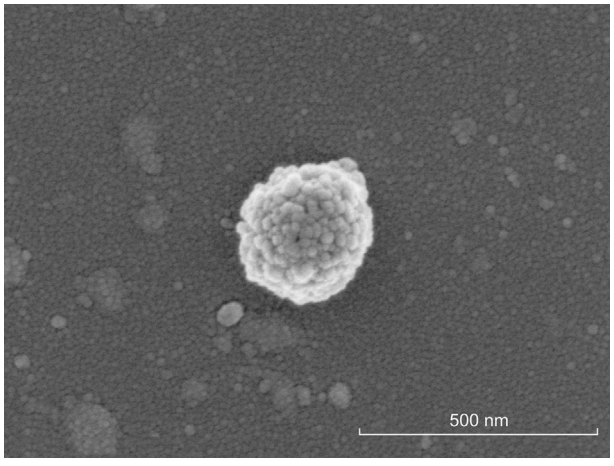

Fig. 3. Scanning electron microscopy (SEM) image of a SC-coupled silica-coated magnetic bead (SMBs).

2.9. Statistical analyses

One-way analysis of variance was performed to determine the statistical significance of the differences between the groups. Statistically significant differences compared with the control group were indicated as $^{*}P < 0.05$, $^{**}P < 0.01$, and $^{***}P < 0.001$. Statistically significant differences between the two contrasting experimental groups were identified as $^{\#}$ for $P < 0.05$, $^{\#\#}$ for $P < 0.01$, and $^{\#\#\#}$ for $P < 0.001$. All statistical analyses were performed using the obtained data ($n \geq 3$) in Origin, Version 2018 (OriginLab, Northampton, MA, USA).

3. Results and discussion

3.1. Expression and purification of His-tagged SC and ST-GFP

Two elution peaks emerged during the linear gradient elution of His-tagged SC (Fig. S1), so the fractions were collected and

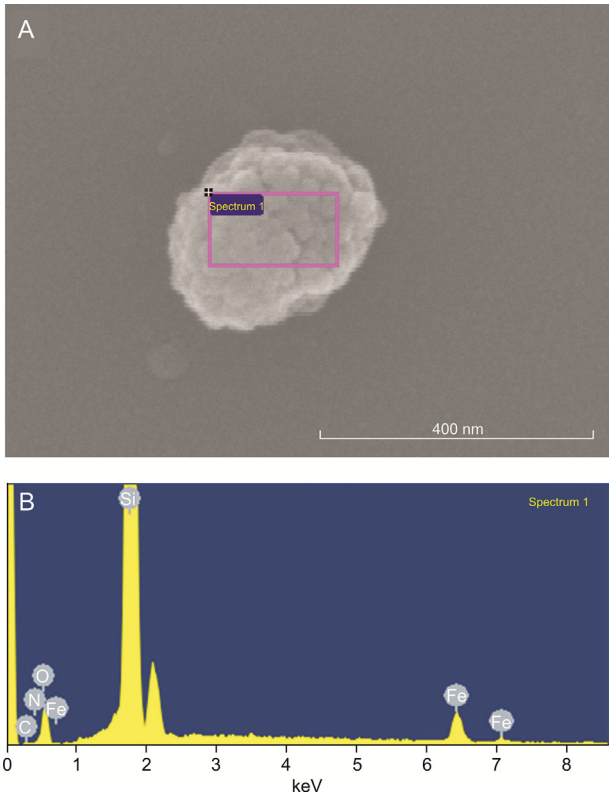

Fig. 4. SEM image and results of energy dispersive spectroscopy (EDS) studies of a SC-SMB. (A) The surface of the bead within the marked analysis region. (B) Corresponding EDS spectrum of a SC-SMB.

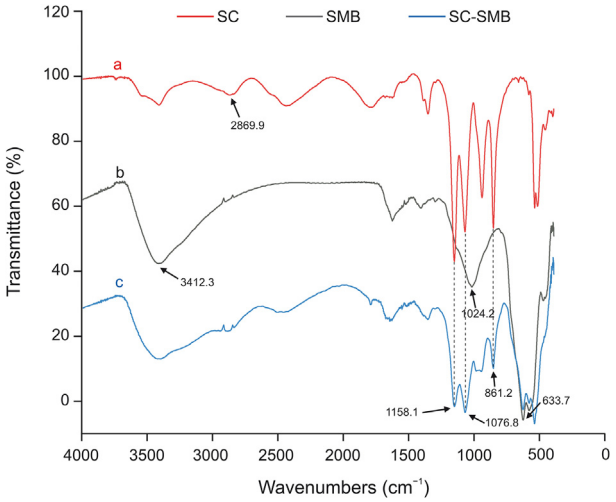

Fig. 5. Fourier transform IR spectra of the (a) purified His-tagged SC, (b) SMBs, and (c) SC-SMBs.

further analyzed via SDS-PAGE. The results showed that the second elution fraction was the purified His-tagged SC (Fig. S2). The purification process for His-tagged ST-GFP was similar to that of SC, and the results were demonstrated via SDS-PAGE (Figs. S3 and S4).

3.2. Confirmation of the spontaneous reaction between SC and ST-GFP

One hundred microliters of the purified His-tagged SC (0.53 mg/mL) and 100 μL of the purified His-tagged ST-GFP (0.19 mg/mL) were mixed and incubated at room temperature for 12 h. The samples were then analyzed via SDS-PAGE (Fig. 1). A clear band of 45 kDa in lanes 5 and 6 were observed (marked by black arrows), indicating that a protein complex close to the expected molecular weight of the SC/ST-GFP complex was formed. As the molar ratio of SC to ST-GFP was 6.27:1, the bands of ST-GFP protein disappeared (marked by white arrows), while a small amount of unreacted SC remained. These results demonstrated that there was indeed a spontaneous reaction [31] between SC and ST-GFP.

To further prove that the bioconjugation between SC and ST-GFP is specific to the cell lysate supernatant, BL-21-SC, and BL-21-ST-GFP cell lysate supernatants were mixed in equal volumes after the optimal induction conditions were applied. The SDS-PAGE results (Fig. S5) demonstrated that the clear bands of 45 kDa in lanes 5 and 6 were observed again (marked by black arrows), indicating that the SC/ST-GFP complex was successfully formed. Meanwhile, by comparison with cell lysate supernatants before mixing, the bands of ST-GFP protein disappeared (marked by white arrows) in lanes 5 and 6, so did those of SC. The results demonstrated that SC and ST-GFP could specifically ligate to each other even when cell lysate supernatants were used. A further test using purified SC mixed with the BL-21-ST-GFP cell lysate supernatant was conducted, and the SDS-PAGE results (Fig. S6) demonstrated that the purified SC could

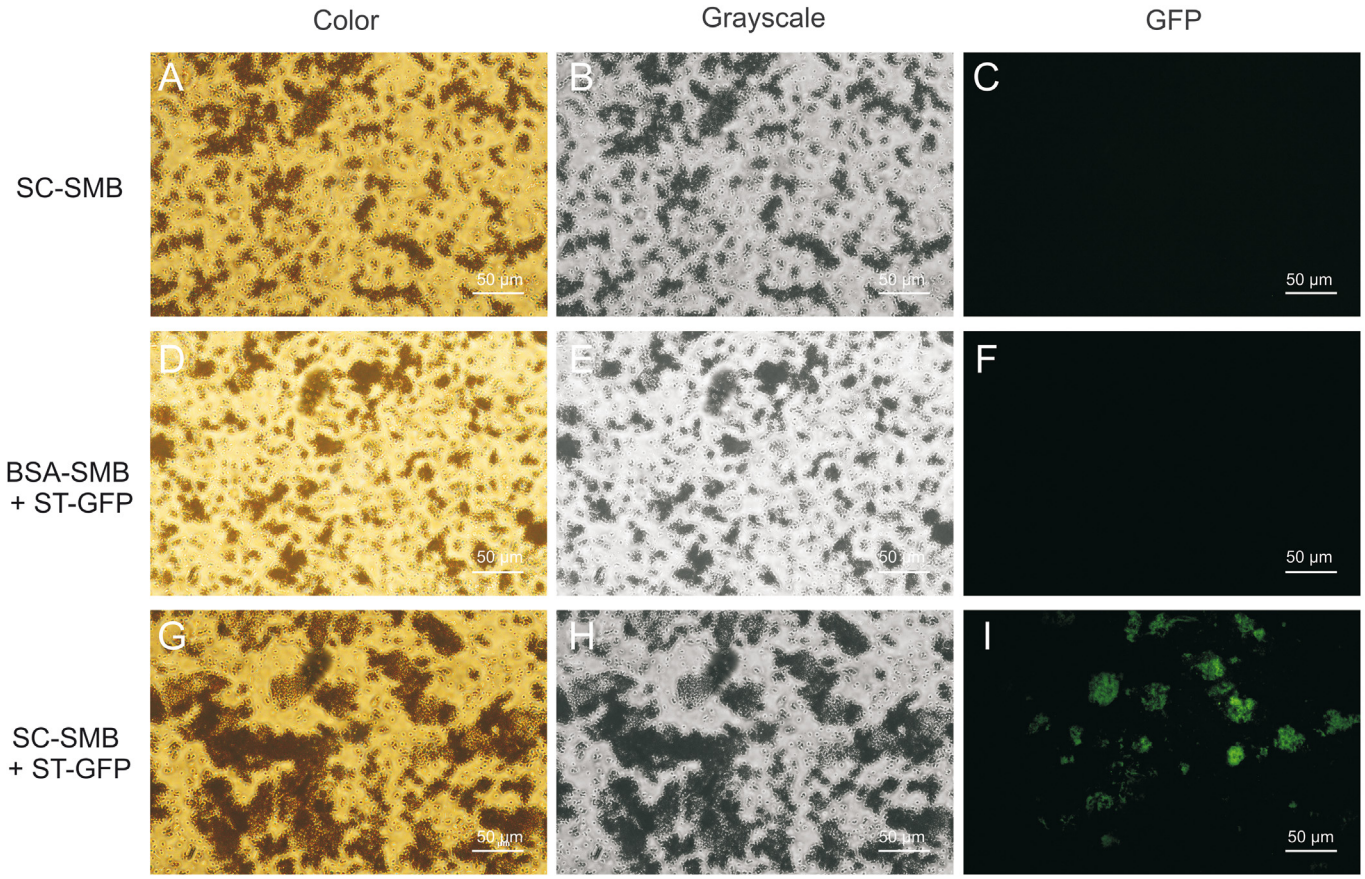

Fig. 6. Fluorescence microscopy images of the different protein-coupled magnetic beads with or without ST-GFP treatment (color, grayscale, GFP). (A–C) Purified His-tagged SC-coupled magnetic beads without ST-GFP treatment (SC-SMBs). (D–F) Bovine serum albumin-coupled magnetic beads treated with ST-GFP (BSA-SMBs + ST-GFP). (G–I) Purified His-tagged SC-coupled magnetic beads treated with ST-GFP (SC-SMBs + ST-GFP).

also specifically capture and ligate ST-GFP from the cell lysate supernatant. We then assessed whether the specificity of the reaction was based on lysine-selectiveness by mixing BSA with the purified ST-GFP overnight (12 h), as numerous lysines exist at various positions within the BSA structure [32]. The SDS-PAGE results (Fig. S7) revealed that no new protein complex was formed in the mixture of BSA and the purified ST-GFP, indicating that the specific bioconjugation between SC and ST-GFP was based on lysine-selectiveness, which may explain the high specificity of this reaction (in vivo and in vitro) [26].

3.3. Characterization of the SC-coupled magnetic beads

We applied this unique self-ligating system to the oriented immobilization of the GFP protein onto SMBs. The first step for this was the preparation of the universal module SC-SMBs, the process of which is shown in Fig. 2.

SEM (×100,000 magnification) and TEM (×40,000 magnification) were performed to characterize the morphology of the SC-coupled magnetic beads. As illustrated by the SEM image in Fig. 3, a layer of homogeneous granules covered the surface of the magnetic bead. Similar results were obtained from the TEM image of the SC-SMBs (Fig. S8), which demonstrated that there were clusters of light-colored granules surrounding the beads. To confirm that the coated granules were indeed proteins, an EDS analysis of the SC-SMBs was carried out (Fig. 4 and Table S1). As shown in Fig. 4B and Table S1, besides elemental Si, Fe, and O, elemental C and N were also detected in the analysis region (Fig. 4A), which indicated that the surrounding granules were proteins, herein considered as purified His-tagged SC.

The FT-IR spectra results (Fig. 5) further proved that the coated proteins on the magnetic beads were indeed SC. The FT-IR spectrum of the SMBs without protein showed three intense peaks at 3412.3 cm^{-1}, 1024.2 cm^{-1}, and 633.7 cm^{-1}, which were attributed to the O—H stretching of carboxylic acids, the asymmetric stretching of the Si—O—Si chain, and the Fe—O stretching vibration of Fe_3O_4, respectively. In the FT-IR spectrum of the purified His-tagged SC, the peak at 2869.9 cm^{-1} represented the symmetric C—H stretching of a methyl group from hydrophobic amino acids, such as alanine, valine, leucine, and isoleucine; the peaks found at 1076.8 cm^{-1} and 1158.1 cm^{-1} were the C—O stretching vibrations of serine (primary alcohol) and threonine (secondary alcohol), respectively; and the peak at 861.2 cm^{-1} represented the out-of-plane C—H bending vibrations of the disubstituted benzene rings from tyrosine. The peaks at 1158.1 cm^{-1}, 1076.8 cm^{-1}, 861.2 cm^{-1}, and 633.7 cm^{-1} were preserved in the FT-IR spectrum of SC-SMBs, indicating that SC proteins were successfully immobilized onto the surface of SMBs.

The CE of SC to the magnetic beads and that of BSA to the magnetic beads were 56.60% and 54.24%, respectively; the RCE of SC to magnetic beads and that of BSA to magnetic beads were 12.00 and 12.80 mg/g, respectively (Table S2).

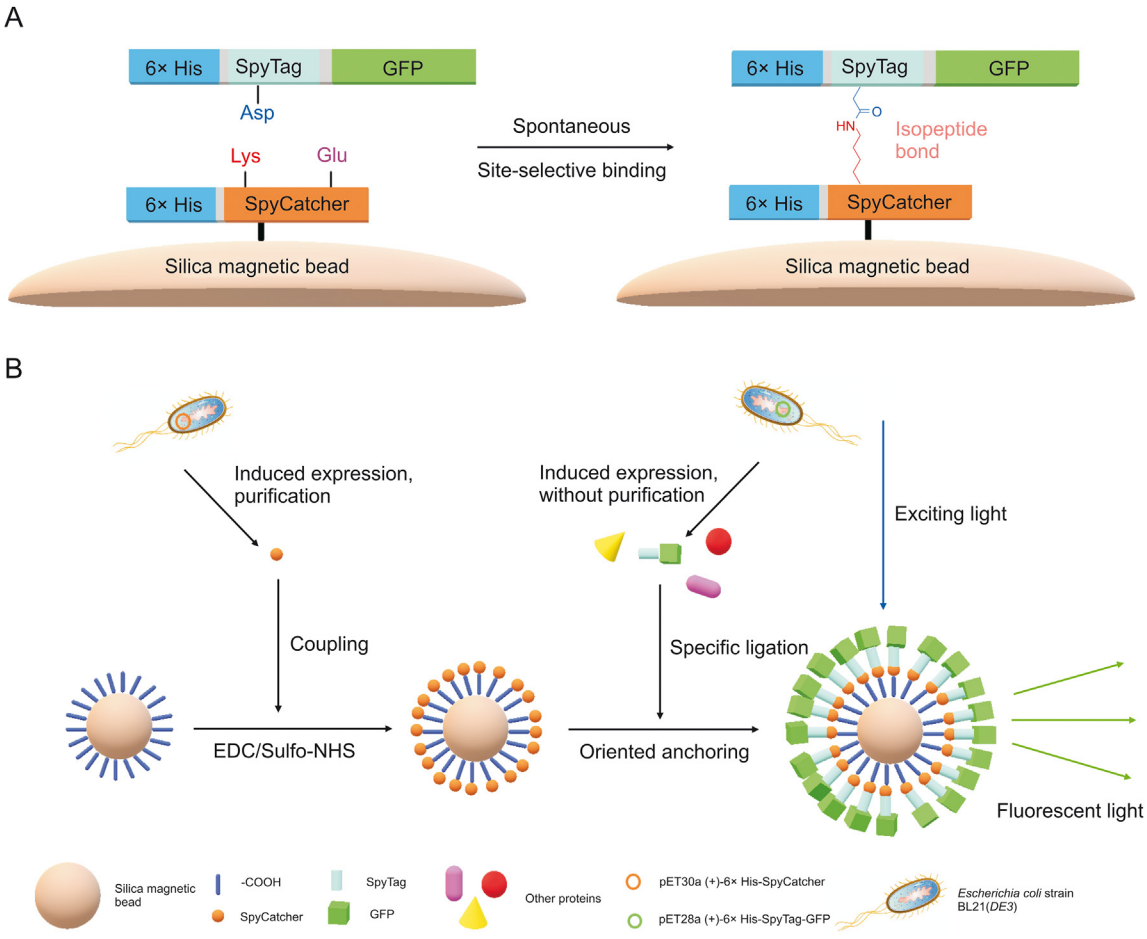

Fig. 7. Preparation and fluorescence imaging schematic diagram of ST-GFP@SC-SMB. (A) Molecular mechanism of the site-selective binding between SC and ST-GFP. (B) Preparation and fluorescence imaging of ST-GFP@SC-SMBs.

3.4. Verification of the oriented immobilization of ST-GFP to the SC-coupled magnetic beads

The SC-SMBs and BSA-SMBs were mixed with the ST-GFP cell lysate supernatant for 12 h, respectively. After rinsing, these beads were observed under bright field (color and grayscale images) and fluorescence microscopy (excitation wavelength range, 460–495 nm, GFP images) at a 400× magnification. The results are presented in Fig. 6. SC-SMBs without ST-GFP treatment served as the blank control (Figs. 6A–C). Green fluorescence was observed in the GFP images of the SC-SMBs treated with ST-GFP (SC-SMBs + ST-GFP) (Fig. 6I). In contrast, there was little green fluorescence in the GFP image of BSA-SMBs treated with ST-GFP (BSA-SMBs + ST-GFP) (Fig. 6F), indicating that although numerous lysines exist in the BSA molecule [32], they could not react with the Asp in ST like the Lys31 in SpyCatcher. Therefore, the highly specific lysine-selective reaction between SC and ST-GFP was again corroborated, and the complete model carrier with fluorescence activity, known as ST-GFP@SC-SMB, was successfully prepared. The preparation and fluorescence imaging schematic diagrams of ST-GFP@SC-SMB are presented in Fig. 7.

3.5. Stability of ST-GFP@SC-SMBs

The alkaline stability of ST-GFP@SC-SMBs was determined together with that of SC-SMBs from the same batch. Both types of beads were treated with 0.1, 0.2, 0.3, 0.4, and 0.5 M NaOH for 2 h, with 0.1 M PBS (pH 7.4)-treated beads serving as the negative control. After the treated beads were separated magnetically, the concentrations of the detached proteins were measured using the Bradford assay. The results are shown in Fig. 8. Specifically, Fig. 8C shows that the concentration of detached proteins from the NaOH-treated ST-GFP@SC-SMBs was significantly higher than that from the 0.1 M PBS-treated beads (pH 7.4) ($P < 0.001$). Meanwhile, in Fig. 8B, the concentration of detached proteins from NaOH-treated SC-SMBs was higher than that from PBS-treated beads ($P < 0.05$). By further comparison of these data, as shown in Fig. 8A, the concentrations of detached proteins measured between the PBS-treated ST-GFP@SC-SMBs and SC-SMBs showed no statistical difference, while the detached protein concentrations measured between ST-GFP@SC-SMBs and SC-SMBs at every NaOH-treated group (0.1–0.5 mol/L) showed significant differences ($P < 0.001$). These results demonstrated that the significant differences ($P < 0.001$) of the detached protein concentrations between NaOH-treated ST-GFP@SC-SMBs and SC-SMBs at each NaOH concentration (0.1–0.5 mol/L) were not caused by PBS treatment (pH 7.4), but the only difference in the experimental conditions, the NaOH treatment, was the most probable reason behind this. To identify the cause of protein detachment, an analysis of the alkaline stability of the complex between SC and ST-GFP was performed. The purified SC and the purified ST-GFP were mixed overnight (12 h) and then treated with PBS or NaOH (0.1–0.5 mol/L) solutions of equal volume for 2 h. The SDS-PAGE results (Fig. S9) showed that both the band of the SC/ST-GFP complex (45 kDa) and the band of excess SC protein smeared after NaOH treatment for 2 h, especially when the NaOH concentration was above 0.2 mol/L. This means that NaOH treatment notably promoted the degradation of the proteins, the mechanism of which might be the amide hydrolysis promoted by hydroxide [33–35]. These results demonstrated that NaOH treatment of ST-GFP@SC-SMBs caused the detachment of proteins from the beads.

The acidic pH stability of the ST-GFP@SC-SMBs was also evaluated. These beads were treated with 0.05 M glycine-HCl buffer (pH 1–6) for 2 h, and the concentration of the detached proteins was measured using the Bradford assay. It can be observed from Fig. S10 that the amount of detached protein from the glycine-HCl buffer-

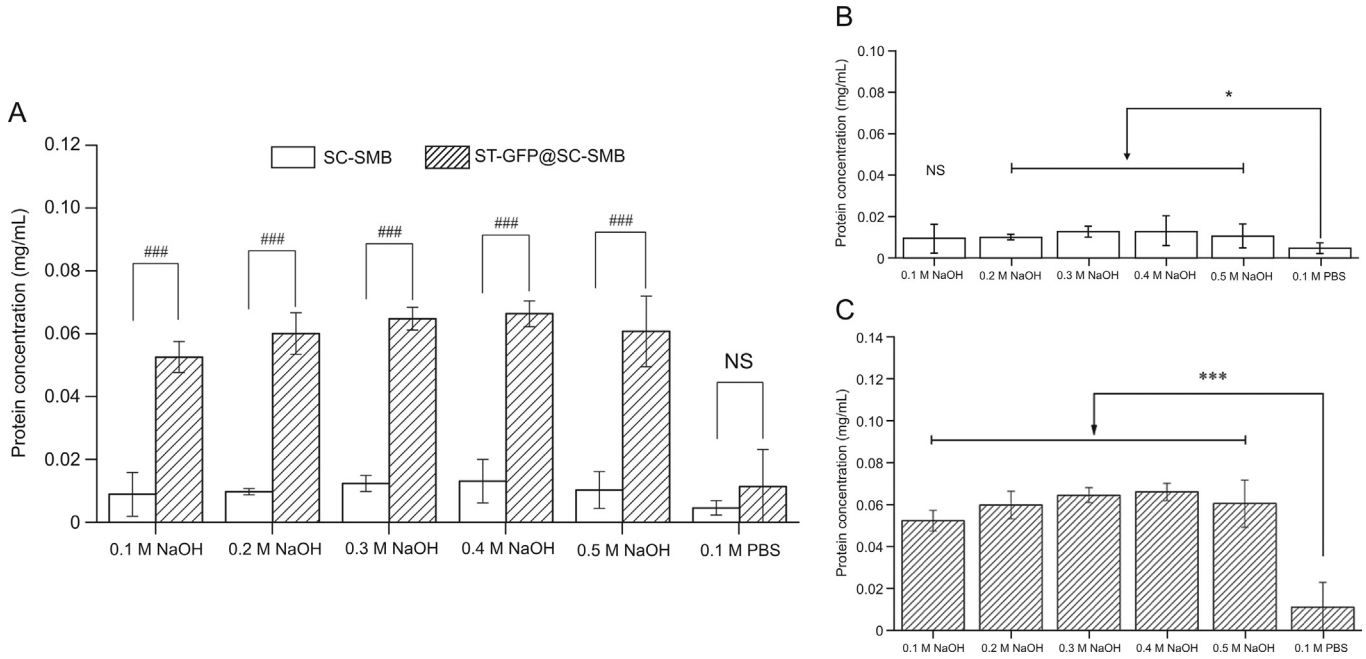

Fig. 8. Alkaline stability of ST-GFP@SC-SMBs and SC-SMBs. All data values represent the mean ± SD ($n = 3$). (A) Comparison of the alkaline stability between SC-SMBs and ST-GFP@SC-SMBs under treatment with the same solution. (B) Alkaline stability of SC-SMBs. (C) Alkaline stability of ST-GFP@SC-SMBs. NS: not significant. $^{###}P < 0.001$. *Significantly different compared to PBS-treated beads, $P < 0.05$. ***Significantly different compared to PBS-treated beads, $P < 0.001$.

treated beads was barely detectable and was not significantly different from that of the beads treated with 0.1 M PBS (pH 7.4) ($P > 0.05$). Therefore, ST-GFP@SC-SMBs were stable in 0.05 M glycine-HCl buffers at all acidic pH values from 1 to 6.

The storage stability of the ST-GFP@SC-SMBs in 20% (*V/V*) ethanol was also examined. The beads were treated with 20% ethanol for up to 7 days, with 0.1 M PBS treatment serving as the negative control. As shown in Fig. S11, the amount of detached protein detected from beads treated with 20% ethanol was slightly lower than that from the beads treated with 0.1 M PBS, but this difference was not significant ($P > 0.05$). Meanwhile, the amount of detached proteins detected from beads treated with 20% ethanol on the seventh day was not significantly different from that on the first day ($P > 0.05$). Hence, ST-GFP@SC-SMBs stored in 20% ethanol exhibited acceptable storage stability for seven days.

The effect of temperature on the stability of ST-GFP@SC-SMBs in 0.1 M PBS (pH 7.4) was also tested. The beads were suspended in 0.1 M PBS (pH 7.4), divided equally, and then incubated in a water bath at different temperatures (4, 25, 37, 45, 55, and 65 °C for 2 h and 100 °C for 10 min). As shown in Fig. S12, there was no significant difference between the amount of detached protein from the 4 °C group and that of the other groups ($P > 0.05$). This means that the ST-GFP@SC-SMBs were stable at most temperatures from 4 to 100 °C. However, considering that protein denaturation might occur at high temperatures, the activity of the immobilized protein was not guaranteed above 37 °C. An operating temperature within 4–37 °C was therefore recommended.

4. Conclusion

In this work, we provided a simple and feasible strategy for the oriented covalent immobilization of proteins onto carboxyl-SMBs directly and selectively from crude cell lysates, which was attributed to the unique self-ligating capability of the ST/SC system. The reaction between SC and ST-GFP was confirmed to be spontaneous and lysine-selective. Although the alkaline stability of ST-GFP@SC-SMBs was not ideal, the isopeptide bond formed was unbreakable in a 0.05 M glycine-HCl buffer (pH 1–6) for 2 h, which was deemed suitable as a potential elution reagent in ligand fishing applications. The excellent stability of ST-GFP@SC-SMBs in a 20% ethanol solution for 7 days demonstrated that 20% ethanol was applicable as a storage reagent for the beads. Despite its good temperature stability, the use of ST-GFP@SC-SMBs within the temperature range of 4–37 °C is recommended.

The bioconjugation between ST and SC was proven to be specific. However, additional non-specific interactions may still exist during ligand or protein fishing experiments. To reduce this, truncated SC sequences [23] can be used, and sequences of both ST and SC can be optimized.

Overall, this preparation method is universal and applicable for various capturing proteins (e.g., receptors, enzymes, antibodies, etc.) that can be genetically encoded and ST-labeled, showing great potential in ligand fishing for applications such as drug discovery and target finding.

CRediT author statement

Yu Yi: Investigation, Conceptualization, Writing - Reviewing and Editing, Data curation; **Jianming Hu**: Investigation, Methodology, Writing - Original draft preparation, Formal analysis, Visualization; **Shenwei Ding**: Investigation, Validation, Software; **Jianfeng Mei**: Writing - Reviewing and Editing, Data curation; **Xudong Wang**: Writing - Reviewing and Editing; **Yanlu Zhang**: Writing - Reviewing and Editing, Data curation; **Jianshu Chen**: Writing - Reviewing and Editing; **Guoqing Ying**: Resources, Project administration, Supervision, Funding acquisition.

Declaration of competing interest

The authors declare that there are no conflicts of interest.

Acknowledgments

The authors thank the College of Pharmaceutical Science, Zhejiang University of Technology, China, for providing the instruments. This work was supported by the Zhejiang Foundation Public Welfare Research Project (Authorization No.: LGF19B060006). We thank the International Science Editing for polishing this manuscript.

Appendix A. Supplementary data

Supplementary data to this article can be found online at https://doi.org/10.1016/j.jpha.2021.07.008.

References

[1] X. Hou, M. Sun, T. Bao, et al., Recent advances in screening active components from natural products based on bioaffinity techniques, Acta Pharm. Sin. B. 10 (2020) 1800–1813.
[2] Y. Fu, J. Luo, J. Qin, et al., Screening techniques for the identification of bioactive compounds in natural products, J. Pharm. Biomed. Anal. 168 (2019) 189–200.
[3] Ł. Cieśla, R. Moaddel, Comparison of analytical techniques for the identification of bioactive compounds from natural products, Nat. Prod. Rep. 33 (2016) 1131–1145.
[4] R. Moaddel, M.P. Marszałł, F. Bighi, et al., Automated ligand fishing using human serum albumin-coated magnetic beads, Anal. Chem. 79 (2007) 5414–5417.
[5] M. Yasuda, D.R. Wilson, S.D. Fugmann, et al., Synthesis and characterization of SIRT6 protein coated magnetic beads: identification of a novel inhibitor of SIRT6 deacetylase from medicinal plant extracts, Anal. Chem. 83 (2011) 7400–7407.
[6] R. Zhuo, H. Liu, N. Liu, et al., Ligand fishing: A remarkable strategy for discovering bioactive compounds from complex mixture of natural products, Molecules 21 (2016) 1516–1532.
[7] J. He, M. Huang, D. Wang, et al., Magnetic separation techniques in sample preparation for biological analysis: A review, J. Pharm. Biomed. Anal. 101 (2014) 84–101.
[8] X.H. Pham, S. Kyeong, J. Jang, et al., Facile method for preparation of silica coated monodisperse superparamagnetic microspheres, J. Nanomater. 2016 (2016), 1730403.
[9] D. Ma, J. Guan, S. Dénommée, et al., Multifunctional nano-architecture for biomedical applications, Chem. Mater. 18 (2006) 1920–1927.
[10] J.H. Jang, H.B. Lim, Characterization and analytical application of surface modified magnetic nanoparticles, Microchem. J. 94 (2010) 148–158.
[11] Y.F. Huang, Y.F. Wang, X.P. Yan, Amine-functionalized magnetic nanoparticles for rapid capture and removal of bacterial pathogens, Environ. Sci. Technol. 44 (2010) 7908–7913.
[12] C.B. Rosen, M.B. Francis, Targeting the N terminus for site-selective protein modification, Nat. Chem. Biol. 13 (2017) 697–705.
[13] C.I. Schilling, N. Jung, M. Biskup, et al., Bioconjugation via azide-Staudinger ligation: an overview, Chem. Soc. Rev. 40 (2011) 4840–4871.
[14] S. Schoffelen, M.B. van Eldijk, B. Rooijakkers, et al., Metal-free and pH-controlled introduction of azides in proteins, Chem. Sci. 2 (2011) 701–705.
[15] A.O. Chan, C.M. Ho, H.C. Chong, et al., Modification of N-terminal α-amino groups of peptides and proteins using ketenes, J. Am. Chem. Soc. 134 (2012) 2589–2598.
[16] E. Haldón, M.C. Nicasio, P.J. Pérez, Copper-catalysed azide-alkyne cycloadditions (CuAAC): An update, Org. Biomol. Chem. 13 (2015) 9528–9550.
[17] B.G. Nidumolu, M.C. Urbina, J. Hormes, et al., Functionalization of gold and glass surfaces with magnetic nanoparticles using biomolecular interactions, Biotechnol. Prog. 22 (2006) 91–95.
[18] S.K. Sahu, A. Chakrabarty, D. Bhattacharya, et al., Single step surface modification of highly stable magnetic nanoparticles for purification of His-tag proteins, J. Nano. Res. 13 (2011) 2475–2484.
[19] Y. Cao, W. Tian, S. Gao, et al., Immobilization staphylococcal protein A on magnetic cellulose microspheres for IgG affinity purification, Artif. Cells Blood Substit. Immobil. Biotechnol. 35 (2007) 467–480.
[20] B. Zakeri, J.O. Fierer, E. Celik, et al., Peptide tag forming a rapid covalent bond to a protein, through engineering a bacterial adhesin, Proc. Natl. Acad. Sci. U S A 109 (2012) E690–E697.

[21] D. Hatlem, T. Trunk, D. Linke, et al., Catching a SPY: Using the SpyCatcher-SpyTag and related systems for labeling and localizing bacterial proteins, Int. J. Mol. Sci. 20 (2019) 2129–2148.
[22] A.H. Keeble, M. Howarth, Power to the protein: Enhancing and combining activities using the Spy toolbox, Chem. Sci. 11 (2020) 7281–7291.
[23] L. Li, J.O. Fierer, T.A. Rapoport, et al., Structural analysis and optimization of the covalent association between SpyCatcher and a peptide Tag, J. Mol. Biol. 426 (2014) 309–317.
[24] B. Zakeri, M. Howarth, Spontaneous intermolecular amide bond formation between side chains for irreversible peptide targeting, J. Am. Chem. Soc. 132 (2010) 4526–4527.
[25] W.B. Zhang, F. Sun, D.A. Tirrell, et al., Controlling macromolecular topology with genetically encoded SpyTag-SpyCatcher chemistry, J. Am. Chem. Soc. 135 (2013) 13988–13997.
[26] A.H. Keeble, M. Howarth, Insider information on successful covalent protein coupling with help from SpyBank, Methods Enzymol. 617 (2019) 443–461.
[27] G.P. Anderson, J.L. Liu, L.C. Shriver-Lake, et al., Oriented immobilization of single-domain antibodies using SpyTag/SpyCatcher yields improved limits of detection, Anal. Chem. 91 (2019) 9424–9429.
[28] W. Ma, A. Saccardo, D. Roccatano, et al., Modular assembly of proteins on nanoparticles, Nat. Commun. 9 (2018), 1489.
[29] M.J.E. Fischer, Amine coupling through EDC/NHS: A practical approach. Surface Plasmon Resonance: Methods in Molecular Biology, Vol. 627, Humana Press, Totowa, New Jersey, 2010, pp. 55–73.
[30] D.A. Morrison, Transformation in *Escherichia coli*: cryogenic preservation of competent cells, J. Bacteriol. 132 (1977) 349–351.
[31] S.C. Reddington, M. Howarth, Secrets of a covalent interaction for biomaterials and biotechnology: SpyTag and SpyCatcher, Curr. Opin. Chem. Biol. 29 (2015) 94–99.
[32] B.X. Huang, H.Y. Kim, C. Dass, Probing three-dimensional structure of bovine serum albumin by chemical cross-linking and mass spectrometry, J. Am. Soc. Mass Spectrom. 15 (2004) 1237–1247.
[33] R.S. Brown, A.J. Bennet, H. Slebocka-Tilk, Recent perspectives concerning the mechanism of H_3O^+- and hydroxide-promoted amide hydrolysis, Acc. Chem. Res. 25 (1992) 481–488.
[34] H. Ślebocka-Tilk, A.A. Neverov, R.S. Brown, Proton inventory study of the base-catalyzed hydrolysis of formamide. Consideration of the nucleophilic and general base mechanisms, J. Am. Chem. Soc. 125 (2003) 1851–1858.
[35] D. Zahn, Car–Parrinello molecular dynamics simulation of base-catalyzed amide hydrolysis in aqueous solution, Chem. Phys. Lett. 383 (2004) 134–137.